Materials Letters 341 (2023) 134250

Contents lists available at ScienceDirect

Materials Letters

journal homepage: www.elsevier.com/locate/matlet

Self-powered white light photodetector with enhanced photoresponse using camphor sulphonic acid treated $CsPbBr_3$ perovskite in carbon matrix

M. Dhakshnamoorthy [a,b], A. Kathirvel [a], S. Mohan Raj [a], Venkata Ramayya Ancha [c], Mulualem Abebe [b], Sudip K. Batabyal [a,d,*]

[a] Department of Science, Amrita School of Physical Sciences, Amrita Vishwa Vidyapeetham, Coimbatore, India
[b] Faculty of Materials Science and Engineering, Jimma Institute of Technology, Jimma University, Jimma, Ethiopia
[c] Faculty of Mechanical Engineering, Jimma Institute of Technology, Jimma University, Jimma, Ethiopia
[d] Amrita Centre for Industrial Research & Innovation (ACIRI), Amrita School of Engineering, Amrita Vishwa Vidyapeetham, Coimbatore, India

ARTICLE INFO

Keywords:
Solar energy materials
Cesium Lead Bromide ($CsPbBr_3$)
Camphor Sulfonic Acid
Carbon materials
Photodetector

ABSTRACT

The surface modification of $CsPbBr_3$ perovskite provides an effective way of defect passivation for device applications. In this work, Camphor sulfonic acid (CSA) was used to modify the surface of $CsPbBr_3$ microcrystals (MCs) and helped in enhancement of Photoluminescence (PL) emission, photoresponse, and photodetectivity. We fabricated the perovskite FTO/c-TiO_2/$CsPbBr_3$-CSA/Carbon composite self-powered photodetector. The device exhibited higher photo responsivity and detectivity of 1.523 mA/W and 2.1454×10^9 Jones, respectively, under white light with excellent stability on high ON/OFF cycles.

1. Introduction

Recently, organic–inorganic halide based perovskite materials with an ABX_3 structure emerged in optoelectronic applications as solar energy materials which includes solar cell, photodetectors, and light emitting diodes [1,2]. Particularly, in photodetectors it has advantages of high optical absorption, long photon-generated charge carrier with high mobility, and readily synthesis methods [3–5]. However, the recombination of the photo-generated charge carriers (electron and hole) limits the performance of perovskite photodetectors. There have been many attempts made by the researchers to improve the performance of photodetectors such as heterostructure and additive modification[6–9]. Though the inorganic perovskite active layer of the photodetector is prepared by simple solution-processed method, it requires expensive electrode with complex preparation method and high energy. Recently, researchers attempted to reduce the cost of the photodetector by using carbon materials based electrodes [10–12]. The surface modification of halide based perovskite materials provides increased absorption of photons and extraction of charge carriers which can enhance the performance of photodetectors [13,14]. The presence of defects on the surface of $CsPbX_3$ microcrystals (MCs) causes charge carrier recombination and reduced performance of photodetector [15]. The surface modification treatment is effectively utilized for passivation of surface defects of $CsPbX_3$ perovskites by introducing ligands during synthesis or post-treatment process [16,17].

In this work, camphor sulfonic acid (CSA) was used the first time to modify the surface of $CsPbBr_3$ perovskite MCs. Binding of the sulfonic acid group with uncoordinated Pb^{2+} on the surface of the $CsPbBr_3$ MCs can increase the photo-emission and stability of $CsPbBr_3$ perovskites. As a result, the surface modification of $CsPbBr_3$ MCs with camphor sulfonic acid enhances the photoresponse and stability.

2. Experimental methods

The perovskite $CsPbBr_3$ MCs were prepared by dissolving 0.3 mmol of CsBr and $PbBr_2$ in 20 mL of DMF solvent under constant stirring. Then, the solution was injected into the 20 mL of toluene containing beaker under vigorous stirring. Immediately, a yellowish colloidal solution formed which indicates the formation of $CsPbBr_3$ microcrystals. The procedure was repeated for the preparation of surface modified $CsPbBr_3$ MCs by adding the Camphor sulfonic acid (CAS) to 0.3 mmol of CsBr/DMF solution. It was observed that CSA modified colloidal solution exhibited enhanced green emission than unmodified solution under UV light irradiation. Finally, the colloidal solutions were centrifuged at 3000 rpm for 10 min and collected precipitates of MCs were dried. The perovskite $CsPbBr_3$/Carbon and $CsPbBr_3$-CSA 20 wt%/Carbon

* Corresponding author at: Department of Science, Amrita School of Physical Sciences, Amrita Vishwa Vidyapeetham, Coimbatore, India.
E-mail address: s_batabyal@cb.amrita.edu (S.K. Batabyal).

https://doi.org/10.1016/j.matlet.2023.134250
Received 23 January 2023; Received in revised form 9 March 2023; Accepted 17 March 2023
Available online 20 March 2023

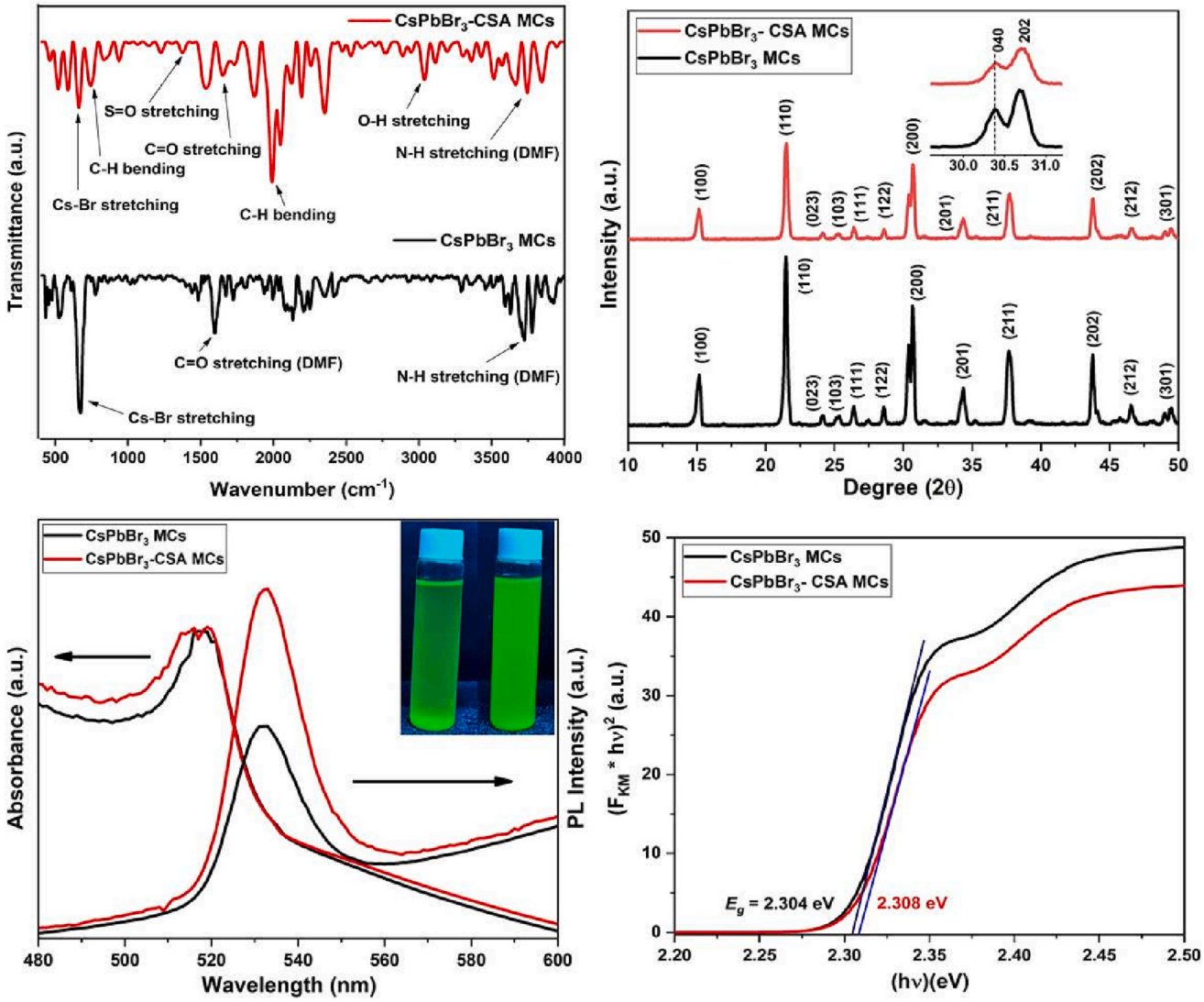

Fig. 1. (a) FTIR spectra, (b) XRD pattern (inset-splitting of the peak at 30°), (c) UV–Visible and PL emission spectra of diluted $CsPbBr_3$ & $CsPbBr_3$-CSA MCs dispersion (inset-image under UV light), and (d) Kubelka-Munk plot of $CsPbBr_3$ and $CsPbBr_3$-CSA MCs.

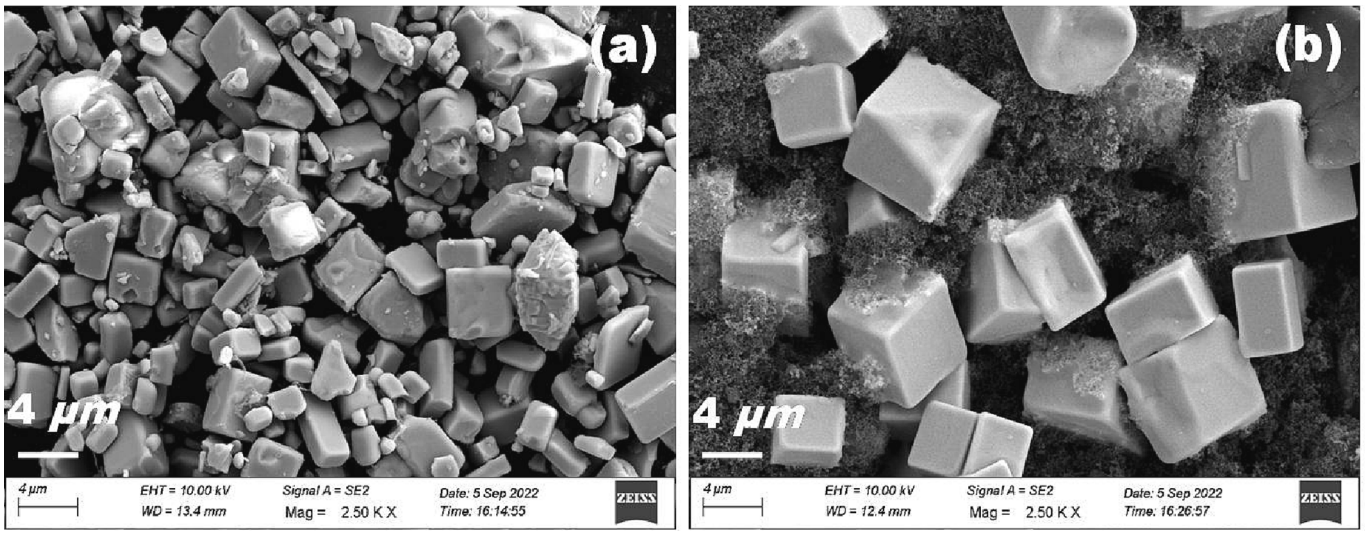

Fig. 2. (a). FE-SEM image of $CsPbBr_3$ and (b). $CsPbBr_3$/CSA/Carbon composite.

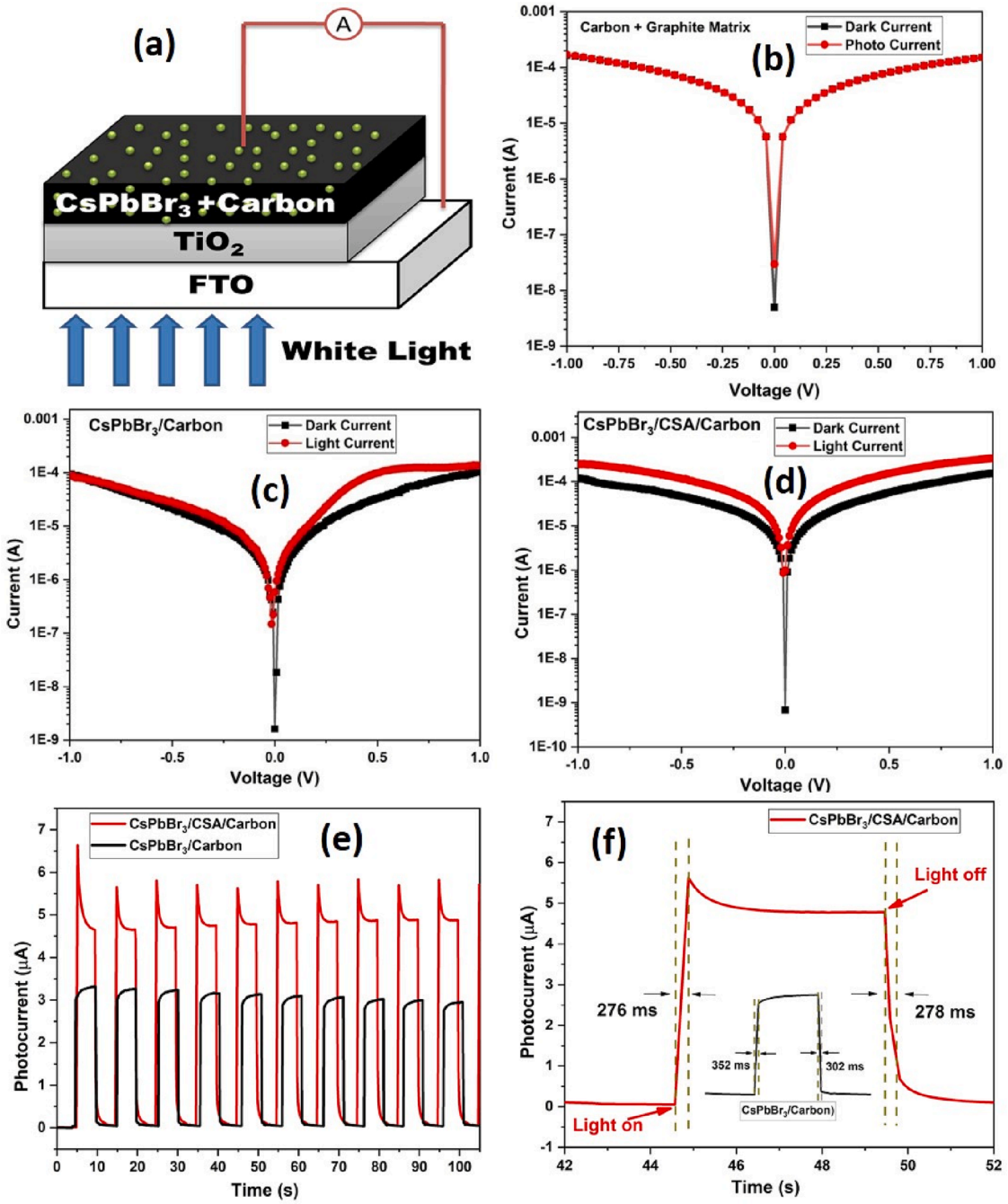

Fig. 3. (a). Schematic diagram of the fabricated Photodetector device, I-V curve of (b) carbon (carbon + Graphite) matrix, (c) $CsPbBr_3$/carbon, (d) $CsPbBr_3$-CSA/carbon, (e). I-t curve, and (f) Rise and decay time (inset-$CsPbBr_3$/Carbon) of Photodetector devices.

composites devices were fabricated according to the reported method [3].

3. Results and discussion

FTIR spectroscopic analysis was conducted using Bruker Alpha-II FTIR spectrometer to confirm the binding of aromatic sulfonic acid with $CsPbBr_3$ microcrystal. Fig. 1(a) shows the FTIR spectra of both samples. The absorption peaks at 1367 cm^{-1}, 3038 cm^{-1}, 1653 cm^{-1} and 745 cm^{-1} attributed to S = O, O–H, C = O stretching bands and C–H in-plane bending vibration which confirm the presence of sulfonic acid. Absorption peaks at 1535 cm^{-1} and 652 cm^{-1} corresponds to aromatic ring and metal halide stretching. The existence of characteristic peaks of aromatic ring and sulfonyl group confirms the successful modification of $CsPbBr_3$ with CSA.

Fig. 1(b) shows the XRD pattern that performed by Rigaku-Ultima-4 X-ray diffractometer (Cu Kα radiation, λ = 1.54 Å). It confirms that both $CsPbBr_3$ and $CsPbBr_3$-CSA MCs are cubic in structure (JCPDS 74–2251). The prominent diffraction peak in the vicinity of 30° (200) splits into two diffraction peaks of (040) and (202), which corresponds to the orthorhombic phase in both $CsPbBr_3$ and $CsPbBr_3$-CSA MCs [7].

Fig. 1(c) shows the UV–Visible absorption and PL spectra which were recorded using Shimadzu 2600 UV–Visible spectrophotometer and spectrofluorophotometer (RF-6000 Spectrofluorophotometer, Shimadzu), respectively by diluting the 0.1 mL reaction product in 5 mL solvent. The absorption peaks at 516 nm were observed and there is no shift in the absorption peak of $CsPbBr_3$-CSA MCs compared to $CsPbBr_3$ MCs. The PL emission spectra show peaks at 531 nm for the excitation

Table 1
Comparison of Photodetector performance between as-fabricated and reported devices.

Type of Device	Rise and Decay Time (τ_r/τ_d) ms	Bias Voltage (V)	Responsivity (A/W)	Detectivity (Jones)	Reference number
FTO/$Cs_3Sb_2Cl_3Br_6$/C	920/700	0	1×10^{-6}	–	[4]
FTO/$Cs_4CuSb_2Cl_{12}$/C/Al	180/120	0	0.17×10^{-3}	3.8×10^{8}	[3]
FTO/$CsPbBr_3$-$SbBr_3$/Al	95/428	0	48.1×10^{-6}	–	[7]
ITO/$CsPbBr_3$-ZnO/Ag	409/17	0	11.5×10^{-3}	–	[6]
FTO/BFO-TU/C	–	0	2.85×10^{-6}	4.06×10^{7}	[8]
FTO/TiO_2/$MAPbI_2$/C	200/500	0	1.3×10^{-3}	8.2×10^{11}	[11]
FTO/TiO_2/$CsPbBr_3$/C	352/302	0	1.003×10^{-3}	1.99×10^{9}	This work
FTO/TiO_2/$CsPbBr_3$-CSA/C	276/278	0	1.523×10^{-3}	2.14×10^{9}	This work

wavelength (FWHM = 21–24 nm) for both $CsPbBr_3$ and $CsPbBr_3$-CSA MCs. The PL emission intensity is significantly increased $CsPbBr_3$-CSA compared to $CsPbBr_3$ MCs. Further, a photographic image of $CsPbBr_3$ and $CsPbBr_3$-CSA MCs colloidal dispersions under UV irradiation (S1) is shown as inset in Fig. 1c. It shows that $CsPbBr_3$-CSA colloidal dispersions is greener and stable even after 5 days than $CsPbBr_3$. The higher stability may be due to the coordination ability of aromatic camphor sulfonic acid with Pb^{2+} which results in the passivation of the surface of $CsPbBr_3$ MCs. The band gap energy is determined by the Kubelka–Munk plot (Fig. 1(d)) [18]. The estimated band gap, E_g = 2.304 and 2.308 eV correspond to $CsPbBr_3$ and $CsPbBr_3$-CSA MCs respectively. The corresponding UV–Visible diffuse reflectance spectrum (by V-750 JASCO UV–VIS spectrophotometer) is given in supplementary information (S2).

The surface morphology of $CsPbBr_3$ MCs and $CsPbBr_3$-CSA/C composite was analyzed from field emission scanning electron microscopic (FE-SEM - Zeiss Merlin Compact instrument) images (Fig. 2). The average size of the formed crystals is in the range from 500 nm to 10 μm. Fig. 2(b) shows the surface morphology of $CsPbBr_3$-CSA MCs reinforced carbon composite and the $CsPbBr_3$-CSA MCs are well embedded in the carbon (carbon + graphite) matrix. Elemental mapping and EDAX table of $CsPbBr_3$-CSA MCs are given in supplementary information (S3).

The schematic of the fabricated carbon based $CsPbBr_3$ perovskite photodetector device is shown in Fig. 3(a). The current–voltage (I-V) characteristics were recorded using a white light source with a keithley2450 instrument under dark and LED light illumination (100 mW/cm^2) for the sweep voltage of −1 to 1 V. Fig. 3(b, c) shows the I-V curves of $CsPbBr_3$/C composite photodetector and there is an increase in photocurrent for $CsPbBr_3$-CSA/C (Fig. 3(d)).

The photo-response of the devices was measured under white light by toggling the light on and off cycle for 5 s. The perovskite $CsPbBr_3$ MCs reinforced carbon (C) composite harvests efficient charges and behaves as a self-powered visible light Photodetector. At zero bias voltage (Fig. 3 (e, f)), the achieved maximum photocurrent was ~6 μA for $CsPbBr_3$-CSA/C whereas $CsPbBr_3$/C attained ~3 μA. I-t curves (S4) at 50 mW/cm^2 light intensity are shown in S5. From the recorded photo-response, the rise & decay time were calculated and given in Table 1. This shows that $CsPbBr_3$-CSA/C device possesses higher stability and excellent photo-response compared to $CsPbBr_3$/C device due to the surface passivation of CSA on $CsPbBr_3$ microcrystals. The higher responsivity of 1.523 mA/W and high detectivity of 2.14×10^9 Jones was achieved for $CsPbBr_3$-CSA/C (Table 1) for 100 mW/cm^2 white light intensity. This is comparably higher than the reported white light based photodetector shown in Table 1.

4. Conclusion

In summary, the current work describes the fabrication of surface modified $CsPbBr_3$ perovskite based carbon composite photodetector by low-cost and simple preparation method. The camphor sulfonic acid (CSA) was used for the defect passivation of $CsPbBr_3$ perovskite microcrystals surface. The presence of CSA was confirmed by FTIR and EDX analysis. Under the light intensity of 100 mW/cm^2 white light irradiation, the fabricated self-powered photodetector showed higher responsivity *(R)* of 1.523 mA/W and detectivity *(D)* of 2.14×10^9 Jones. This provides feasible application of surface modification on perovskite material based photodetectors.

CRediT authorship contribution statement

M. Dhakshnamoorthy: Conceptualization, Methodology, Validation, Formal analysis, Investigation, Writing – original draft. **A. Kathirvel:** Validation, Visualization, Writing – review & editing. **S. Mohan Raj:** Validation, Writing – review & editing. **Venkata Ramayya Ancha:** Resources, Writing – review & editing. **Mulualem Abebe:** Resources, Writing – review & editing. **Sudip K. Batabyal:** Conceptualization, Resources, Investigation, Project administration, Supervision, Writing – review & editing.

Declaration of Competing Interest

The authors declare that they have no known competing financial interests or personal relationships that could have appeared to influence the work reported in this paper.

Data availability

Data will be made available on request.

Acknowledgement

Authors extend their gratitude to Centre for ExiST project: Excellence in Science & Technology – Ethiopia (funded by KfW, Germany), and Jimma Institute of Technology, Jimma University.

Appendix A. Supplementary data

Supplementary data to this article can be found online at https://doi.org/10.1016/j.matlet.2023.134250.

References

[1] M. Xue, H. Zhou, G. Ma, L. Yang, Z. Song, J. Zhang, H. Wang, Sol. Energy Mater. Sol. Cells. 187 (2018) 69–75, https://doi.org/10.1016/j.solmat.2018.07.023.
[2] R. Chen, Z. Liang, W. Feng, X. Hu, A. Hao, J. Alloys Compd. 864 (2021), 158125, https://doi.org/10.1016/j.jallcom.2020.158125.
[3] P.M. Jayasankar, A.K. Pathak, S.P. Madhusudanan, S. Murali, S.K. Batabyal, Mater. Lett. 263 (2020), 127200, https://doi.org/10.1016/j.matlet.2019.127200.
[4] A.K. Pramod, M. Raj Subramaniam, S.A. Hevia, S.K. Batabyal, Mater. Lett. 306 (2022), 130874, https://doi.org/10.1016/j.matlet.2021.130874.
[5] X. Song, F. Wang, H. Zhang, H. Li, Z. Xu, D. Wei, J. Zhang, Z. Dai, Y. Ren, Y. Ye, X. Ren, J. Yao, Mater. Lett. 326 (2022) 3–6, https://doi.org/10.1016/j.matlet.2022.132909.
[6] C. Li, C. Han, Y. Zhang, Z. Zang, M. Wang, X. Tang, J. Du, Sol. Energy Mater. Sol. Cells. 172 (2017) 341–346, https://doi.org/10.1016/j.solmat.2017.08.014.
[7] M.R. Subramaniam, A.K. Pramod, S.A. Hevia, S.K. Batabyal, S.K. Batabyal, J. Phys. Chem. C. 126 (2022) 1462–1470, https://doi.org/10.1021/acs.jpcc.1c07493.
[8] A. Kathirvel, A. Uma Maheswari, S.K. Batabyal, M. Sivakumar, Mater. Lett. 284 (2021), 128906, https://doi.org/10.1016/j.matlet.2020.128906.
[9] Y. Che, X. Cao, L. Du, Z. Zhu, J. Zhang, Opt. Mater. (Amst). 127 (2022), 112279, https://doi.org/10.1016/j.optmat.2022.112279.
[10] X. Tang, Z. Zu, Z. Zang, Z. Hu, W. Hu, Z. Yao, W. Chen, S. Li, S. Han, M. Zhou, Sensors Actuators, B Chem. 245 (2017) 435–440, https://doi.org/10.1016/j.snb.2017.01.168.

[11] S. Murali, S.P. Madhusudanan, A.K. Pathak, P.M. Jayasankar, S.K. Batabyal, Mater. Lett. 254 (2019) 428–432, https://doi.org/10.1016/j.matlet.2019.07.105.
[12] Z. Li, S.A. Kulkarni, P.P. Boix, E. Shi, A. Cao, K. Fu, S.K. Batabyal, J. Zhang, Q. Ziong, L. Wong, N. Mathews, S.G. Mhaisalkar, ACS Nano. 8 (2014) 6797–6804.
[13] J. Qiu, W. Xue, W. Wang, Y. Li, Dye. Pigment. 198 (2022), 109806, https://doi.org/10.1016/j.dyepig.2021.109806.
[14] B. Yang, W. Bi, F. Jin, X. Ma, S.Q. Guo, Compos. Commun. 29 (2022), 101032, https://doi.org/10.1016/j.coco.2021.101032.
[15] S. Seth, T. Ahmed, A. De, A. Samanta, ACS Energy Lett. 4 (2019) 1610–1618, https://doi.org/10.1021/acsenergylett.9b00849.
[16] Z. Shen, S. Zhao, D. Song, Z. Xu, B. Qiao, P. Song, Q. Bai, J. Cao, G. Zhang, W. Swelm, Small. 16 (2020) 1–28, https://doi.org/10.1002/smll.201907089.
[17] F. Krieg, S.T. Ochsenbein, S. Yakunin, S. Ten Brinck, P. Aellen, A. Süess, B. Clerc, D. Guggisberg, O. Nazarenko, Y. Shynkarenko, S. Kumar, C.J. Shih, I. Infante, M. V. Kovalenko, ACS Energy Lett. 3 (2018) 641–646, https://doi.org/10.1021/acsenergylett.8b00035.
[18] T.K. Athira, M. Roshith, R. Kadrekar, A. Arya, M.S. Kumar, G. Anantharaj, L. Gurrala, V. Saranyan, S.B. TG, V.R.K. Darbha, Mater. Res. Express. 7 (2020) 104002. https://doi.org/10.1088/2053-1591/abbdeb.